PHYSICAL REVIEW B VOLUME 31, NUMBER 4 15 FEBRUARY 1985

Surface dipole and Fermi-level position on clean, oxygen-, and water-covered cylindrical Si crystals: A photoelectron spectroscopy study

W. Ranke
Fritz-Haber-Institut der Max-Planck-Gessellschaft, Faradayweg 4-6, 1000 Berlin 33, West Germany

Y. R. Xing
Semiconductor Institute, Chinese Academy of Sciences, P.O. Box 650, Beijing, People's Republic of China

(Received 9 August 1984)

Photoelectron spectroscopy, including emission from the Si $2p$ core level, was used to investigate the orientation dependence of the photoionization threshold $\xi(\alpha)$ and the surface position of the valence-band edge below the Fermi level, $E_{\mathrm{VFS}}(\alpha)$, on a cylindrically shaped Si crystal with $[1\bar{1}0]$ as its axis. The average ξ values for (001), (113), (111), and (110) are 5.33, 5.32, 5.26, and 5.26 eV, respectively, and thus differ only very little as expected for a covalent, nonpolar crystal. Increasing corrugation on stepped, faceted, defect-rich, and high-index surfaces increases ξ values, in contrast to what is observed on metal surfaces. The orientation dependence of ξ is interpreted in terms of a relaxation- or reconstruction-related surface polarity which is increased at edges. Water adsorption generally reduces ξ. In the range (001)—(113) the shape of $\xi(\alpha)$ is conserved, whereas it is changed in the range (112)—(111)—(110), consistent with fundamentally different adsorption mechanisms as observed earlier. After oxygen adsorption, $\xi(\alpha)$ is strongly changed, indicating a strong distortion of the surface by bond breaking. On the clean surface, the Fermi-level—pinning position $E_{VFS}(\alpha)$, which is given by the surface-state structure, varies strongly. After oxygen exposure it is pinned at a nearly constant position ~ 0.1 eV above the midgap, probably by defect-related surface states. For water adsorption, again two ranges can be distinguished with a similar pinning as for oxygen in the range (112)—(111)—(110) and a reduced but still strong variation between (001) and (113).

I. INTRODUCTION

It has been known for a long time that the surface-dipole barrier in solids should vary with orientation. Already in 1941, Smoluchowsky proposed the so-called charge-smoothing model, which qualitatively explains the variations of the work function φ on metals.[1] According to this model, which was the basis for the more recent theoretical work of Lang and Kohn,[2] the electronic charge at a solid surface tends to smooth out corrugations, yielding a work-function decrease with increasing corrugation. Systematic experimental work has started relatively late, and because of increasing interest in the structural and chemical properties of vicinal and high-index surfaces.[3] An elegant work on that topic is a measurement of $\varphi(\alpha)$ on a complete tungsten cylinder by Gardiner *et al.*[4] All these measurements confirm the idea of charge smoothing as being mainly responsible for the orientation dependence of the surface dipole on metals.

Charge smoothing implies that the electronic charge can be shifted easily and thus is expected to be strong for metals. The situation is more complicated for covalent crystals, which are characterized by strongly directed bonds with strongly localized orbitals. For compound crystals, ionic contributions to the electron affinity χ (which, for semiconductors, is the quantity containing the surface-dipole contributions) must be considered. Measurements on a cylindrical GaAs crystal[5] have shown that the bulk ionicity as reflected in the surface composition gives the main contribution to $\chi(\alpha)$. However, the surface ionicity is reduced compared to the bulk, which is related to the reconstruction of the surface atoms.

In view of these results, it seemed interesting to investigate $\chi(\alpha)$ on a nonpolar covalent crystal, and Si was chosen for this purpose. Charge smoothing should be small and thus ionicity contributions could originate only from surface-relaxation and reconstruction effects. Thus, it was hoped that such measurements also could explain the general relaxation mechanisms.

This paper is organized as follows. After the description of experimental details and sample preparation in the next section, Sec. III presents the experimental results, e.g., the temperature and orientation dependence of the ionization threshold $\xi=\chi+E_G$ (E_G is the energy gap) and the Fermi-level position in the band gap, as well as their change upon oxygen and water adsorption. The paper is concluded by a discussion of these results in Sec. IV.

II. EXPERIMENTAL AND DATA EVALUATION

The cylindrical sample was cut by spark erosion from a 0.1-Ω cm boron-doped p-type Si disk supplied by Wacker Chemitronic, Burghausen, West Germany. After cutting, it was mounted on a turning lathe and polished at low rotation speed, simultaneously moving the polishing cloth to and fro, parallel to the rotation axis. In this way, the preferential formation of polishing grooves along the sample perimeter could be avoided, resulting in a perfect mirror-like surface. The axis of the cylinder [Fig. 1(a)] was $[1\bar{1}0]$, so that all the main low-index orientations and all

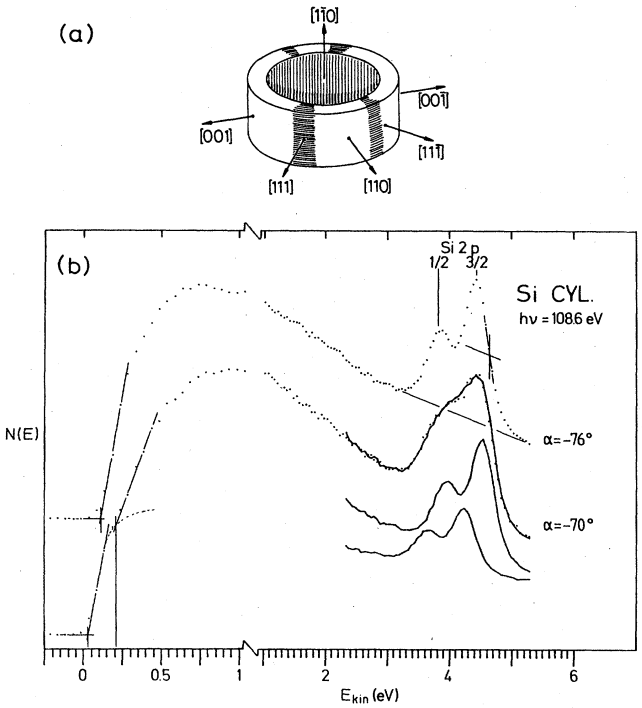

FIG. 1. (a) The ring-shaped cylindrical sample with the main low-index orientations. (b) Examples of photoemission spectra. At $\alpha=76°$, the spectrum shows well-separated Si $2p$ spin-orbit-split peaks. At $\alpha=70°$, the Si $2p$ emission is smeared and two low-energy thresholds are observed, indicating an overlap of emission from two domains. The spectrum can be fitted by two contributions of the shape of the spectrum at $\alpha=-76°$ (solid line).

intermediate-index orientations were displayed on its surface. The cylinder height was 10 mm and its diameter 23 mm. It was ring shaped, and the heater (W wire on a ceramic support) was placed inside the sample.

In this way, a homogeneous temperature and a relatively low loss of heating power was achieved. The sample holder (similar to that described in Ref. 6) consisted of Ta, and a maximum temperature of 1200 K could be reached.

A Pt-PtRh thermocouple was attached to the sample holder at a place where the glowing color was similar to that of the sample. The precision of the temperature reading, therefore, is estimated to be ±25 K. To avoid preferential etching effects, the sample was not chemically etched but directly cleaned in ultrahigh vacuum (UHV) by cycles of Ar^+ bombardment and annealing (1050—1100 K). In the early stages of cleaning, a Cu contamination of up to ~3% of a monolayer (ML) was observed, probably from an out-diffusing bulk contamination which caused a (6×6) superstructure on (111). Finally, this contamination was below the Auger detection limit of ~0.005 ML. Carbon contamination was in the same range. To accelerate the cleaning procedure, sputtering of the sample with higher ion energy (4 keV) at elevated temperature (1100 K) was attempted. However, this resulted in the formation of a tarnished (matte) surface at all but some low-index orientations. After this the sample was freshly polished and sputtered at room temperature (RT) and energies not above 1 keV. Gases (triply-distilled water and 99.998%-pure O_2, respectively) were introduced via leak valves. The ionization gauge was switched on during admission.

The measurements were performed in a stainless-steel UHV chamber containing low-energy electron-diffraction (LEED) optics, an ion gun, and a double-pass cylindrical mirror analyzer (CMA) for Auger-electron (AES) and ultraviolet photoelectron spectroscopy (UPS). Light from the Berlin synchrotron source BESSY, in connection with the monochromator SX-700 incident at an angle of 60° with respect to the sample normal, was used. The width of the light beam at the sample was 0.3 mm, thus averaging over an orientation range of about 3° on the curved sample surface. Owing to the larger LEED primary-beam diameter (~1 mm), its orientation resolution was only about 5°.

On semiconductors, the variation of the surface dipole with orientation or upon adsorption is reflected in the variation of the electron affinity $\chi=E_{vac}-E_C$ (E_{vac} is the vacuum energy level; E_C is the conduction-band edge) or in the ionization threshold $\xi=E_{vac}-E_V$ (E_V is the valence-band edge). Both values differ only by the energy-gap value $E_G=E_V-E_C$. Since E_G is temperature dependent and since E_V is directly accessible in photoemission, we evaluate ξ as a measure for the surface dipole.

The ionization threshold ξ is given by $\xi=h\nu-W$. W is the total width of the spectrum, corrected by an appropriate analyzer-resolution term. The low-energy (secondary-electron) cutoff is steep and easy to determine [see Fig. 1(b), upper curve]. On Si, the high-energy edge [valence-band (VB) edge] overlaps with strong emissions from orientation-dependent surface states.[7] It is therefore necessary to measure the position of a sharp, bulk, core-level-derived structure whose binding energy (E_B^V) relative to E_V is known. We used the spin-orbit-split Si $2p$ core levels as reference levels [Fig. 1(b)], with $E_B^V=-98.74$ eV for Si $2p_{3/2}$ at (001) (Ref. 8). To minimize the known surface core-level contributions,[9] $h\nu=108.6$ eV was used so that the Si $2p$ emission appeared at $E_{kin}\sim4$ eV, where the electron escape depth is of the order of 50 Å, and thus quite large.[10] The most precise reference was not the position of the maximum of the $2p$ peak, but the half-height position of its high-energy slope, which was as sharp as the low-energy cutoff, yielding a relative error of ±15 meV for ξ. The position of the high-energy reference gives, at the same time, the relative position of E_V with respect to the Fermi level E_F at the surface, $E_{VFS}=(E_V-E_F)_{surf}$, which, in this way, can be evaluated with an even lower relative error of ±10 meV.

Since neither the Si, $2p$ binding energy nor the value of $h\nu$ is known with comparable precision, the absolute calibration of ξ and E_{VFS} was performed using the following values from Ref. 11: $\varphi=4.63$ eV and $E_F-E_V=0.65$, and thus $\xi=5.28$ eV for Si(111)-(7×7); and $\varphi=4.87$ eV and $E_F-E_V=0.46$ eV, and thus $\xi=5.33$ eV for Si(001)-(2×1).

For most orientations, the Si $2p$ emission was well resolved, as for $\alpha=-76°$ in Fig. 1(b). Only in the ranges (115)—(113) and (11$\bar{5}$)—(11$\bar{3}$) was it smeared, obviously due to the overlap of domains of different E_{VFS} and ξ. In addition, the low-energy edge showed two thresholds there, as is shown for $\alpha=-70°$ in Fig. 1(b). However, the Si $2p$ emission could mostly be fitted excellently by two contributions of the shape of the spectrum at $\alpha=-76°$, yielding E_{VFS} and the relative intensity of both domains. The low-energy edge could be separated less precisely, so that the relative error of ξ in these ranges was of the order of ± 30 meV.

Water has a high sticking coefficient below ~ 400 K, especially at and near (001).[12,13] It affects ξ, as will be shown in detail. Since water is always a component of the residual gas, the measuring time between cleaning cycles was limited to between 30 and 60 min, depending on the orientation, before adsorbate-induced changes were observable. On the other hand, it turned out, as will also be shown, that on (001) ξ is temperature dependent, so that measurements could be started only after cooling below ~ 400 K, which took ~ 20 min with our large and temperature-inert sample and holder. After a period of 30—60 min, the sample was heat-cleaned again and the measurement continued. The reproducibility of the absolute values of ξ and E_{VFS} for different preparation cycles was typically ± 20 and sometimes ± 60 meV at maximum. The reproducibility of the orientation dependence, i.e., the shape of $\xi(\alpha)$ and $E_{VFS}(\alpha)$, was much better.

III. RESULTS

A. Temperature dependence of ξ at (001)

Figure 2 shows the change of ξ and E_{VFS} during cooldown of the heat-cleaned sample. The sample temperature and the total residual-gas exposure is shown as well. At (00$\bar{1}$), ξ decreases strongly between $T=550$ and ~ 400 K, followed by a weaker decrease which has not yet finished after 45 min (~ 320 K). Temperature increase above 550 K increases ξ. However, the initial value is not reached. E_{VFS}, to the contrary, remains constant until, after ~ 30 min, the temperature is below 350 K, and only then does it drop slowly. At $\alpha=-62°$ [between (11$\bar{3}$) and (33$\bar{7}$)], only a quite slow decrease of ξ is observed. E_{VFS} remains constant as for (00$\bar{1}$). The strong decrease at (00$\bar{1}$) between 550 and 400 K is interpreted to be due to a temperature-dependent change in the surface-dipole moment probably caused by a structural phase transition. Below ~ 400 K, the (001)-specific water adsorption[13,14] can occur, which reduces ξ further. That adsorption from the residual gas cannot be responsible for the first fast decrease follows from the constant value of E_{VFS}, which should decrease both by H_2O and O_2 adsorption (see Sec. III C). As expected for water adsorption, E_{VFS} starts to decrease only around 350 K. Warming up to ~ 550 K increases ξ by ~ 130 meV, which corresponds to the value of the fast decrease. That the initial value is not reached is consistent with adsorption of a certain amount of water which is dissociated to form atomically adsorbed oxygen at that temperature.[13] Thus the phase transition appears to be reversible. Although this phenomenon was not studied in detail, on other orientations no indications of a similar behavior were noticed.

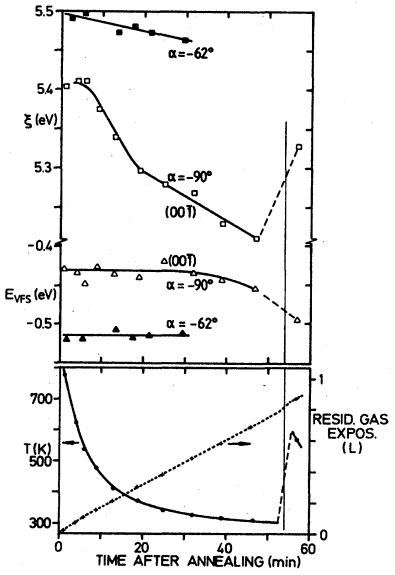

FIG. 2. Change of ξ and E_{VFS} with time after heat cleaning. For (00$\bar{1}$) the decrease of ξ is strongly temperature dependent. The sample temperature and the total residual-gas exposure in langmuirs (1 L$\hat{=}10^{-6}$ Torr sec) are also shown (lower panel).

It is interesting to compare this result with the LEED investigations of Olshanetsky and Mashanov,[15] who have observed several order-order transitions on (110) and order-disorder transitions on many other orientations. However, on (001) no such transition occurred. We therefore must conclude that the transition observed here is not connected with a change of the surface periodicity.

B. ξ and E_{VFS} of the clean sample

The orientation dependence of ξ and E_{VFS} of the clean sample is displayed in Figs. 3—5. The values from different preparation cycles (freshly sputtered and annealed,

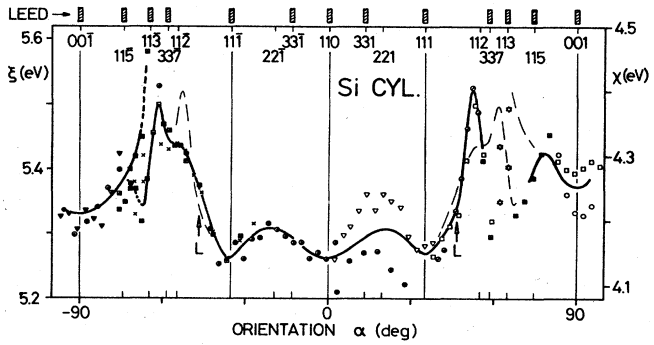

FIG. 3. Orientation dependence of the ionization threshold ξ on clean Si. Identical symbols indicate measurements within the same preparation cycle. The right-hand scale gives the electron affinity χ using a gap value $E_G=1.12$ eV (Ref. 24). The orientations where clear nonfaceted and nonstepped LEED patterns were observed are marked at the top edge of the figure.

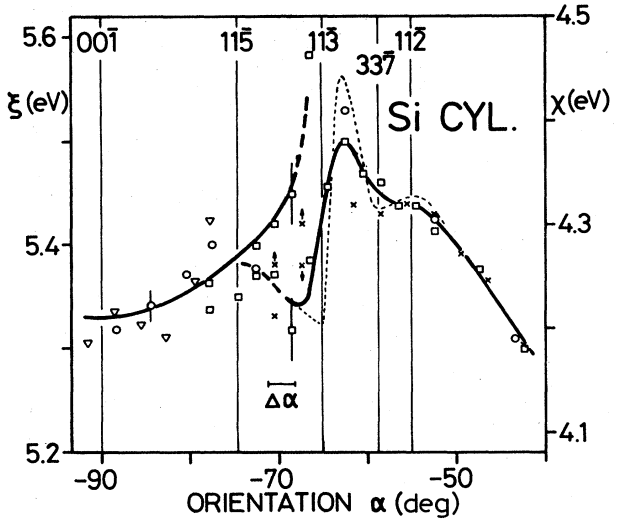

FIG. 4. Same as Fig. 3, expanded scale. The dotted curve represents a qualitative correction for the orientation resolution $\Delta\alpha$.

or only annealed) are marked by different symbols. As seen, e.g., between (110) and (111) the absolute values may differ for different preparations by up to ~80 meV. The variation with orientation, however, is very well reproducible. The thick solid line gives the average of the measured points. Between (11$\bar{5}$) and (11$\bar{3}$), the energy-distribution curves (EDC's) consisted of two overlapping spectra which could be deconvoluted as described in Sec. II. Correspondingly, the curves are split there, with the dashed parts indicating the respective minority contributions. Also, around (113), overlapping spectra were observed. However, their separation was not as easy, possibly because of the overlap of more than two components. Therefore we did not attempt to plot an average curve in that range.

In general, the symmetry of the crystal structure is reflected in $\xi(\alpha)$ (Fig. 3) and E_{VFS} (Fig. 5). $\xi(\alpha)$ has minima at (110), (111), and (11$\bar{1}$) and at (001) and (00$\bar{1}$). Between (00$\bar{1}$) and (11$\bar{1}$), as well as (111) and (001), the behavior is complicated and somewhat different for both ranges. Thus, near (112) towards (111) ($\alpha=52°$), a clear, sharp maximum appears, whereas at the corresponding orientation at $\alpha=-52°$, only a shoulder is found. To accentuate differences, the corresponding symmetrical curves are plotted as dashed lines for comparison.

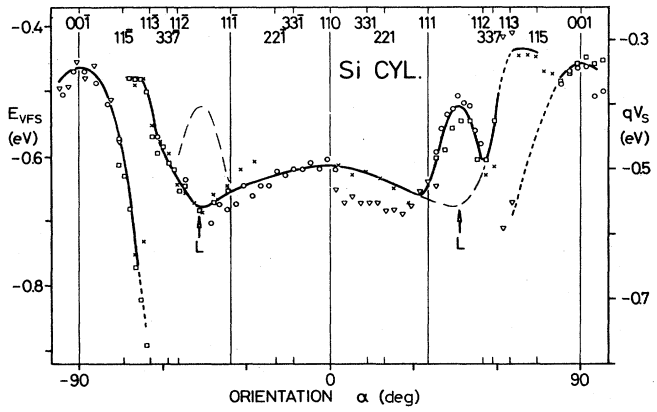

FIG. 5. Orientation dependence of the surface valence-band position below E_F, $E_{VFS}(\alpha)$. Identical symbols indicate measurements within the same preparation cycle. The right-hand scale gives the corresponding band bending.

The strongly structured region between (11$\bar{2}$) and (00$\bar{1}$) is plotted on an expanded scale in Fig. 4. The error bars and the orientational resolution $\Delta\alpha$ due to the finite light-spot size are indicated. Owing to this $\Delta\alpha$, the sharp structures are smeared and a correction for the orientational resolution was attempted (dotted line). This corrected curve shows that ξ has a minimum at (11$\bar{3}$), and probably also at (33$\bar{7}$), whereas near $-52°$ a small maximum would appear at the position where the strong maximum was found at $\alpha=+52°$. The minima at (11$\bar{3}$) and (33$\bar{7}$) correspond to clear and facet-free LEED structures which were observed there. Although the orientational resolution in LEED is worse, $\Delta\alpha=5°$, than for UPS, the LEED structure observed near (11$\bar{2}$) must be ascribed to (33$\bar{7}$) because the found periodicity (unit-cell size) fits precisely to (33$\bar{7}$) and not to (11$\bar{2}$).[16]

Also in the plot of E_{VFS} (Fig. 5), the general symmetry of the crystal is seen, apart from the regions (111)—(112) and (11$\bar{1}$)—(11$\bar{2}$). Between (112) and (115), the situation is less confusing than for ξ, because in the evaluation of E_{VFS} only the variation of the high-energy edge (or the Si $2p$ binding energy, respectively) is involved, whereas for ξ the low-energy cutoff is also used. On the right-hand abscissa, the band bending qV_s is also given, which is related to E_{VFS} by the known position of E_F in the bulk, which is 0.12 eV above E_V.

C. ξ and E_{VFS} after adsorption

In Fig. 6 the change of ξ after exposure to 10 L O_2 and 2 L H_2O at 350 K is displayed (1 L=1 langmuir=10^{-6} Torr sec). The dashed line gives the clean-surface curve, for comparison. ξ is generally reduced by water adsorption, most strongly between (00$\bar{1}$) and (11$\bar{2}$). Between (00$\bar{1}$) and (11$\bar{3}$) the shape of the curve is preserved, including the splitting between (11$\bar{5}$) and (11$\bar{3}$). This is different for O_2 adsorption. The splitting is eliminated and, at (00$\bar{1}$), ξ is unchanged although oxygen is adsorbed. Also in the range (11$\bar{2}$)—(11$\bar{1}$)—(110), the shape has changed strongly, indicating a strong disturbance of the surface structure by adsorption. In this range, both the O_2 and H_2O curves are similar in shape, indicating a similar influence on the surface structure.

The change of the surface Fermi-level position E_{VFS} by adsorption is shown in Fig. 7. Between (11$\bar{2}$) and (110), the adsorbate influence is weak, indicating no strong changes in the E_F pinning position. Between (00$\bar{1}$) and (11$\bar{2}$), the strong structures of the clean surface are preserved, but reduced in amplitude by water, whereas they are completely removed by oxygen. In general, E_{VFS} tends to move towards a value of -0.65 eV for all orientations, which corresponds to a Fermi-level position approximately 0.1 eV above midgap.

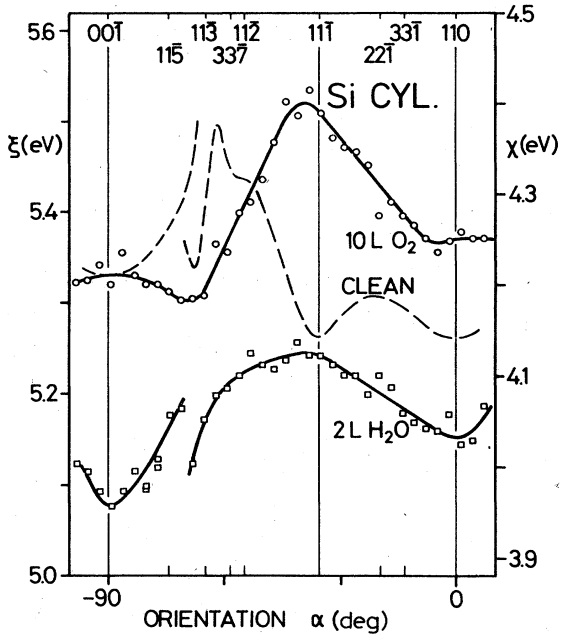

FIG. 6. Orientation dependence of the ionization threshold ξ after exposure to oxygen and water, respectively. 1 L$\hat{=}10^{-6}$ Torr sec.

IV. DISCUSSION

According to the symmetry of the bulk crystal structure of Si, the plots of ξ and E_{VFS} (Figs. 3 and 5) should be symmetrical with respect to (110). In general, this is observed apart from the regions between $\alpha=\pm 85°$ and $\pm 40°$. We attribute the differences in these regions to differences of facet and/or step sizes. Within the shown cycle of measurements, the differences generally appeared

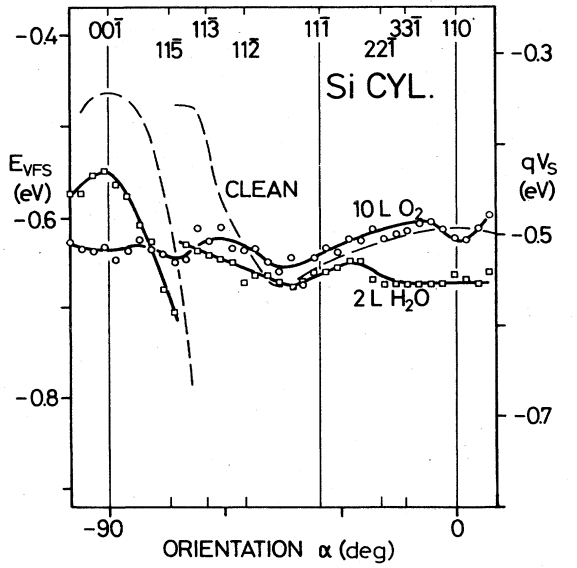

FIG. 7. Orientation dependence of the surface valence-band position below E_F, $E_{VFS}(\alpha)$, after exposure to oxygen and water, respectively. 1 L$\hat{=}10^{-6}$ Torr sec.

reproducible, but with small variations. Thus the shoulder in ξ around $\alpha=-52°$ (Fig. 3) sometimes was more pronounced, or even formed a small maximum. In addition, the sharpness of the peak at $\alpha=-62°$ varied somewhat from preparation to preparation. As will be discussed below, more open or stepped regions have higher ξ values, so that high maxima, as at $\alpha=+52°$, are an indication of stepped surfaces or small facets, whereas at the corresponding orientation at $\alpha=-52°$, probably larger facets were formed. The general behavior towards step and facet formation may depend on random differences during initial sample preparation. That such differences in facet formation actually exist was observed by the use of LEED at $\alpha=\pm 47°$ at the positions marked L in Figs. 3 and 5. At $\alpha=+47°$, spots originating from (111)-(7×7) facets were observed which were missing at $\alpha=-47°$. These (7×7) facets correlate with an increase of ξ near (111) towards (112) which is more gradual than that from (11$\bar{1}$) towards (11$\bar{2}$). Even more pronounced differences for both these orientations are seen in E_{VFS} (Fig. 5).

In general, if facets are thermodynamically favorable with respect to steps, their formation still is greatly influenced, and may be hindered, by the problem of transporting Si atoms across the surface by diffusion. The resulting surface structure may be far from equilibrium and may consist of a mixture of facets of different kind and size. This is obviously the case around (113), whereas the situation is clearer around (11$\bar{3}$). Here, ξ as well as E_{VFS} can well be separated into the contribution from two kinds of facets. Near (001), steps two atomic layers high are formed (Refs. 17 and 18, and our own LEED observation). Starting from (00$\bar{1}$), ξ increases and E_{VFS} decreases continuously with step concentration until, near (11$\bar{3}$), these stepped facets form the minority contributions, which finally disappear. Starting at $\sim$(11$\bar{5}$), these steps begin to bunch into (11$\bar{3}$)-like facets, quickly forming the majority contribution (best seen in the resolution-corrected curve in Fig. 4) when approaching the (11$\bar{3}$) minimum of ξ.

In Fig. 3 the orientations are indicated where clean, ordered, and unfaceted LEED patterns were observed.[16] At all these orientations, ξ has a minimum. Only at (11$\bar{5}$) could a minimum not be resolved. The orientations where the LEED pattern was easiest to obtain are (001), (113), (111), and (110). Their ξ values are very similar, differing only by $\sim$70 meV. Since the orientation variation of the surface dipole on a nonpolar covalent crystal can originate only from relaxation- and/or edge-related dipole contributions, this small variation suggests similar principal relaxation mechanisms for all stable surface configurations on the different orientations. The argument can be reversed: Stable surface structures are found only where the possible relaxation mechanism finds a structure which geometrically fits well with the given bulk geometry.

On (001) the most widely accepted relaxation model is that of the asymmetric dimer first proposed by Chadi.[19] As pointed out by Pauling and Herman,[20] from a more chemical point of view, this model means that half the surface atoms which are protruding from the surface rehybridize from the sp^3 state in the bulk towards a trivalent p^3-like state which would have a lone s^2 pair if

the ideal configuration could be achieved. The charge would originate from the other half of the atoms, which would assume a more sp^2-like, nearly flat configuration. In this way, a surface dipole is formed with the negative side up, thus increasing ξ with respect to a nonrelaxed configuration. The similarity of ξ on all stable surfaces suggests that such a relaxation-induced dipole contribution exists everywhere, so that the possibility of a similar rehybridization should be considered for structure models on all surfaces.

However, such rehybridizations are possible for many different models. Thus all structural models consistent with the tunneling microscopy model of Binnig *et al.*[21] for Si(111)-(7×7) contain atoms protruding from the surface, thus tending to assume a p^3 configuration, and atoms tending to assume a flat sp^2-like configuration can be found which would be consistent with the similar values of ξ found in this work.

Starting from the low-index orientations $(00\bar{1})$, $(11\bar{3})$, $(33\bar{7})$, $(11\bar{1})$, and (110), ξ increases. These deviations are connected with an increasing number of atomic steps [near $(00\bar{1})$ (Refs. 17 and 18), and by our own observation, near (111) towards (110) (Ref. 17)] or disorder and facets. In any case, the number of edge atoms is increased. We interpret the increase of ξ to be due to an easier and thus stronger relaxation along edges, which thus leads to an increased dipole contribution. The possibility of such an edge-related dipole is demonstrated in Fig. 8 for a step from (001) towards (113). On the (001) terraces, the asymmetric dimer relaxation[19] is assumed. The step is two atomic layers high.[17,18] Atom 1 is expected to rehybridize toward a flat sp^2 configuration into the direction indicated by an arrow. This affects the position of the surrounding atoms, and atom 2 can improve its p^3 character. A charge shift from atom 1 to atom 2 will be connected with this rehybridization, thus generating an additional dipole, which increases ξ.

Between $(00\bar{1})$ and $(11\bar{2})$, water adsorption leaves the shape of $\xi(\alpha)$ essentially unchanged, lowering it, however, by 0.2—0.3 eV. UPS carried out on the valence-band region shows that in this range the predominantly adsorbed species is the same as has been observed at (001).[13,14] The conservation of the shape of $\xi(\alpha)$ indicates an interaction without destruction of the surface structure by backbond breaking. This observation is consistent with dissociation into OH and H groups adsorbed on top and saturating the Si dangling bonds as proposed by Ibach *et al.*,[12] but also with molecular adsorption as proposed by Schmeisser *et al.*[14] Both OH and H_2O, adsorbed with the oxygen end toward the Si substrate, also can account for the observed decrease of ξ. Between $(11\bar{2})$ and (110), the shape of $\xi(\alpha)$ is similar to that of adsorbed oxygen. In this range, only a small portion of H_2O is adsorbed in the form as an (001), whereas most of it dissociates to O and/or OH species.[13] Simultaneously, backbonds are broken as in the case of oxygen adsorption.[22] Thus the similarity of the shape of $\xi(\alpha)$ after O_2 and H_2O exposure in this orientation range is understandable. We ascribe the lower value after H_2O adsorption to the small portion of the species as found on $(00\bar{1})$, which was ascribed to adsorption on microscopically (001)-like defect sites or facets.[13]

Between $(00\bar{1})$ and $(11\bar{2})$, O_2 adsorption changes $\xi(\alpha)$ completely as well. Simultaneous Si $2p$ core-level-shift measurements[22] showed that oxygen had partly penetrated into the lattice [most strongly at $(11\bar{1})$, and most weakly at $(11\bar{3})$ and (110)]. Thus $\xi(\alpha)$ qualitatively follows the strength of interaction and surface destruction, and no longer reflects the clean-surface structure. The nearly constant position of E_F after oxygen adsorption (Fig. 7) confirms this. The destructive interaction of oxygen [and also water between $(11\bar{2})$ and (110)] creates extrinsic surface states which pin E_F nearly independent of orientation.

Finally, in Fig. 9, the orientation dependence of ξ on clean Si is compared to that of the polar semiconductor GaAs,[23] and to the work function of a metal (tungsten).[4]

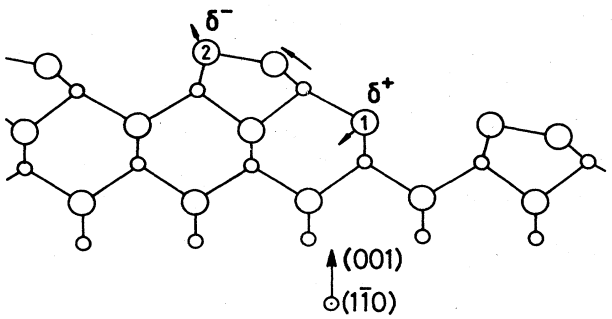

FIG. 8. Relaxation change along a (001)—(111) edge and corresponding dipole formation. For (001) the asymmetric dimer relaxation (Ref. 19) is assumed.

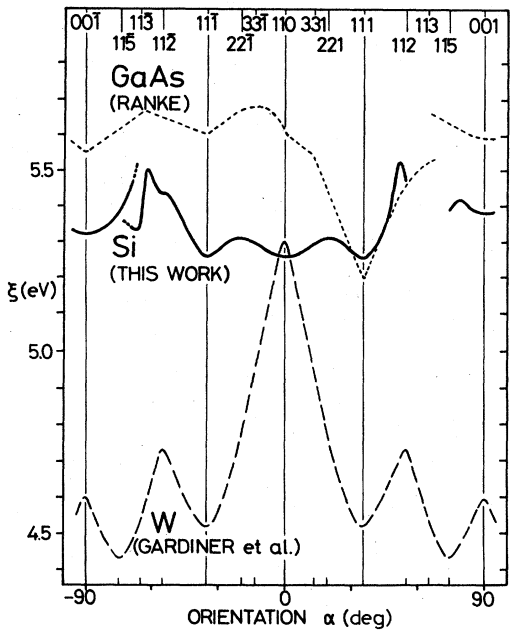

FIG. 9. Comparison of the orientation dependence of the work function of tungsten (Ref. 4) with the ionization threshold of GaAs, prepared by molecular-beam epitaxy (Refs. 5 and 23), and of Si (this work).

All measurements were performed using cylindrical samples. The GaAs curve shown is for preparation by molecular-beam epitaxy (MBE), which yields As-rich phases on (001) [$c(2\times8)$] and (11$\bar{1}$) [(2×2)].[25]

Gardiner *et al.*[4] have interpreted the work-function variation $\varphi(\alpha)$ in terms of the "charge-smoothing" effect,[1,2] which yields a decrease of φ for more open (stepped or corrugated) structures with respect to close-packed surfaces. In fact, the expected corrugation on a body-centered-cubic crystal as W varies precisely in the order given by $\varphi(\alpha)$ from (110) (close packed) over (112)—(001)—(111) to (115).

The asymmetry of the GaAs curve with respect to (110) already indicates that the surface stoichiometry plays an essential role: Ideally, (11$\bar{1}$) would be As-terminated, whereas (111) is Ga-terminated. The known relaxation at (110) (Ref. 26) moves surface As atoms outward and Ga atoms inward, and at (00$\bar{1}$) and (001) the surface is As-rich after MBE preparation. Thus the polarity of the crystal with As (Ga) bearing an excess negative (positive) charge determines $\xi(\alpha)$, whereas charge smoothing plays, if any, a minor role. It is interesting that the variation of surface stoichiometry with (111) and (11$\bar{1}$) as extrema yields a smaller variation than the charge-smoothing contribution for W. The reason is that surface-relaxation or -reconstruction effects, which are generally strong on semiconductor surfaces, and polarity effects, are not independent. Relaxation, in general, will be connected with a rehybridization, and thus with charge redistribution. Therefore the polarity of surface atoms, in general, is expected to be reduced with respect to the bulk.[5] Obviously, the surface relaxes in a way which simultaneously reduces the number of dangling bonds (e.g., by rehybridization) and the polarity.

Si has no intrinsic polarity. Consequently, the variations of $\xi(\alpha)$ still are smaller than for GaAs and amount to only $\frac{1}{3}$ to $\frac{1}{4}$ of the variation on W. However, the variations are generally the opposite of what would be expected from charge-smoothing effects. Instead of decreasing, ξ increases with step concentration. That charge-smoothing effects are weak follows from the covalent character of the bond. The electronic charge is strongly located in directed bonds, unlike the much less structured electron clouds in a more or less free-electron-like metal. Instead, the surface atoms relax, forming rehybridized bonds to reduce the number of dangling bonds. Every rehybridization, however, must change the charge distribution and thus the polarity. In the case of a III-V compound such as GaAs, the surface atoms can rehybridize and, at the same time, decrease their polarity. On the Si surface, however, polarity is induced, creating a dipole contribution, which is the reason for the orientation dependence of ξ.

A low polarity and, at the same time, a relaxation which geometrically fits the bulk periodicity below, is a strong requirement which often is satisfied by the formation of very large surface unit cells [e.g., Si(111)-(7×7) and GaAs(111)-($\sqrt{19}\times\sqrt{19}$)R23.4°]. In certain orientation ranges it can obviously not be satisfied and facets are formed. This explains the split of $\xi(\alpha)$ for Si between (11$\bar{5}$) and (11$\bar{3}$). The formation of facets from an originally more or less statistically rough, polished and sputtered surface is a transport problem of atoms across the surface. Thus it is not surprising that the thermodynamically most stable configuration is not always established. The unresolved mixture of different facet contributions for Si around (113) is therefore understandable.

Generally, we can conclude that the charge-smoothing effect which essentially determines $\varphi(\alpha)$ on metals[1–4] is weak or negligible on crystals with preferentially covalent-bond character. Instead, relaxation and reconstruction effects and the resulting polarity changes give the main contributions. On compounds such as GaAs, the main contribution originates from the crystal polarity,[5] although it is reduced with respect to the bulk. On nonpolar crystals such as Si, the amplitude of the $\xi(\alpha)$ variation is comparatively small and given by relaxation-induced dipole moments or, in other words, by a relaxation-induced surface polarity.

ACKNOWLEDGMENTS

The support by the staff of the Berlin synchrotron radiation source BESSY, especially A. Puschmann, J. Haase, and H. Petersen, is gratefully acknowledged. Thanks are due H. Haak for sample preparation.

[1]R. Smoluchowski, Phys. Rev. **60**, 661 (1941).
[2]N. D. Lang and W. Kohn, Phys. Rev. B **3**, 1215 (1971).
[3]For a review, see H. Wagner, in *Solid Surface Physics*, Vol. 85 of *Springer Tracts in Modern Physics*, edited by G. Höhler (Springer, Berlin, 1979).
[4]T. M. Gardiner, H. M. Kramer, and E. Bauer, Surf. Sci. **112**, 181 (1981).
[5]W. Ranke, Phys. Rev. B **27**, 7807 (1983).
[6]W. Ranke, Y. R. Xing, and G. D. Shen, Surf. Sci. **120**, 67 (1982).
[7]J. E. Rowe and H. Ibach, Phys. Rev. Lett. **32**, 421 (1974); F. J. Himpsel, Th. Fauster, and G. Hollinger, Surf. Sci. **132**, 22 (1983); W. Ranke and D. Schmeisser, *ibid.* (to be published).
[8]F. J. Himpsel, G. Hollinger, and R. A. Pollak, Phys. Rev. B **28**, 7014 (1983).
[9]F. J. Himpsel, P. Heimann, T.-C. Chiang, and D. E. Eastman, Phys. Rev. Lett. **45**, 1112 (1980).
[10]M. P. Seah and W. A. Dench, Surf. Interface Anal. 1, 2 (1979).
[11]G. Hollinger and F. J. Himpsel, J. Vac. Sci. Technol. A **1**, 640 (1983).
[12]H. Ibach, H. Wagner, and D. Bruchmann, Solid State Commun. **42**, 457 (1982).
[13]W. Ranke and D. Schmeisser, Surf. Sci. (to be published).
[14]D. Schmeisser, F. J. Himpsel, and G. Hollinger, Phys. Rev. B **27**, 7813 (1983).
[15]B. Z. Olshanetsky and V. I. Mashanov, Surf. Sci. **111**, 414 (1981).
[16]Y. R. Xing and W. Ranke (unpublished).
[17]B. Z. Olshanetsky and A. A. Shklyaev, Surf. Sci. **82**, 445

(1979).
[18]R. Kaplan, Surf. Sci. **93**, 145 (1980).
[19]D. J. Chadi, Phys. Rev. Lett. **43**, 43 (1979).
[20]L. Pauling and Z. S. Herman, Phys. Rev. B **28**, 6154 (1983).
[21]G. Binnig, H. Rohrer, C. Gerber, and E. Weibel, Phys. Rev. Lett. **50**, 120 (1983).
[22]A detailed analysis of the adsorption-induced Si $2p$ core-level shifts will be published elsewhere.
[23]Used were the original data from which the χ values of Ref. 5 were calculated. In Ref. 5 an energy-gap value, $E_G = 1.35$ eV, was used, which is too small by 0.07 eV (Ref. 24). A thorough reexamination of the original data, including a more precise consideration of the analyzer resolution, resulted in a further decrease of all χ values by 0.1—0.15 eV. The variation of χ with orientation is not affected.
[24]S. M. Sze, *Physics of Semiconductor Devices* (Wiley, New York, 1981).
[25]W. Ranke and K. Jacobi, Prog. Surf. Sci. **10**, 1 (1981).
[26]C. B. Duke, Appl. Surf. Sci. **11-12**, 1 (1982), and references cited therein.